Sizing optimization of sandwich plate with laminate faces

E. Kormanikova and K. Kotrasova

***Abstract*—**The paper is focused on sandwich optimization subjected to the maximum displacement criterion. The optimization problem is based on the use of continuous design variables. Thicknesses of layers with the known layer orientation are used as design variables. The optimization problems with displacement constraints are formulated to minimize the sandwich weight. The designs of the final thickness of sandwich plate have to be rounded off to integer multiples of the commercially available layer thickness.

***Keywords*—**Design optimization, displacement criterion, sandwich structure, thickness design variable, weight objective function.

I. Introduction

The typical sandwich structure consists of three layers. The outer layers are made of high strength material such as steel, fiber reinforced laminates etc., which can transfer axial forces and bending moments, while the core is made of lightweight materials such as foam, alder wood etc. The material used in sandwich core must be resistant to compression and capable of transmitting shear [1].

The design optimization problem of current interest is the minimization of the weight function for a sandwich composite plate. This is a design optimization problem which optimizes the thickness of the composite laminae and core to give the minimum weight. A greater interest to current study is given to the works on the design optimization of composite plates where the thicknesses are taken as the design variables.

A symmetric sandwich plate to the mid-plane has the objective function of minimizing the weight function. As design variables are used thicknesses of layers and are computed using the Sequential Linear Programming method. Within this method the Modified Feasible Direction method was used.

The optimization of a composite plate is important analysis for design of structures ranging from aircrafts to civil engineering structures [2-4].

Eva Kormanikova is with the Department of Structural Mechanics, Institute of Structural Engineering, The Technical University of Kosice, Faculty of Civil Engineering, Vysokoskolska 4, 042 00 Kosice, Slovak Republic (e-mail: eva.kormanikova@tuke.sk).

Kamila Kotrasova is with the Department of Structural Mechanics, Institute of Structural Engineering, The Technical University of Kosice, Faculty of Civil Engineering, Vysokoskolska 4, 042 00 Kosice, Slovak Republic (corresponding author to provide phone: +421 55 6024294; e-mail: kamila.kotrasova@tuke.sk).

II. Effective Moduli of Composites

If the composite has periodic microstructure, then Fourier series can be used to estimate all the components of the stiffness tensor of a composite. Explicit formulas for a composite reinforced by long circular cylindrical fibres, which are periodically arranged in a square array (Fig. 1) are written in the following way.

Because the microstructure has square symmetry, the stiffness tensor has six unique coefficients given by [5]

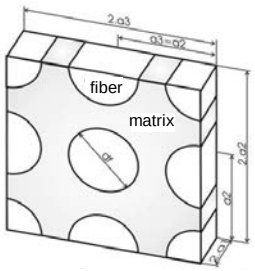

Fig. 1 periodic square microstructure model

$$C_{11}=\lambda^{(m)}+2\mu^{(m)}-\frac{\xi}{D}\left(\frac{S_3^2}{\mu^{(m)2}}-\frac{2S_6S_3}{\mu^{(m)2}g}-\frac{aS_3}{\mu^{(m)}c}+\frac{S_6^2-S_7^2}{\mu^{(m)2}g^2}+\frac{aS_6+bS_7}{\mu^{(m)}gc}+\frac{a^2-b^2}{4c^2}\right) \tag{1}$$

$$C_{12}=\lambda^{(m)}+\frac{\xi}{D}b\left(\frac{S_3}{2c\mu^{(m)}}-\frac{S_6-S_7}{2c\mu^{(m)}g}-\frac{a+b}{4c^2}\right) \tag{2}$$

$$C_{22}=\lambda^{(m)}+2\mu^{(m)}-\frac{\xi}{D}\left(-\frac{aS_3}{2\mu^{(m)}c}+\frac{aS_6}{2\mu^{(m)}gc}+\frac{a^2-b^2}{4c^2}\right) \tag{3}$$

$$C_{66}=\mu^{(m)}-\xi\left(-\frac{S_3}{\mu^{(m)}}+\left(\mu^{(m)}-\mu^{(f)}\right)^{-1}\right)^{-1} \tag{4}$$

$$C_{23}=\lambda^{(m)}+\frac{\xi}{D}\left(\frac{aS_7}{2\mu^{(m)}gc}-\frac{ba+b^2}{4c^2}\right) \tag{5}$$

$$C_{44}=\mu^{(m)}-\xi\left(\frac{2S_3}{\mu^{(m)}}+\left(\mu^{(m)}-\mu^{(f)}\right)^{-1}+\frac{4S_7}{\mu^{(m)}\left(2-2\nu^{(m)}\right)}\right)^{-1} \tag{6}$$

where

$$D=\frac{aS_3^2}{2\mu^{(m)2}c}-\frac{aS_6S_3}{\mu^{(m)2}gc}+\frac{a\left(S_6^2-S_7^2\right)}{2\mu^{(m)2}g^2c}+\frac{S_3\left(b^2-a^2\right)}{2\mu^{(m)}c^2}+ \\ +\frac{S_6\left(a^2-b^2\right)+S_7\left(ab+b^2\right)}{2\mu^{(m)}gc^2}+\frac{\left(a^3-2b^3-3ab^2\right)}{8c^3} \quad (7)$$

$$a=\mu^{(f)}-\mu^{(m)}-2\mu^{(f)}\nu^{(m)}+2\mu^{(m)}\nu^{(f)} \quad (8)$$

$$b=-\mu^{(m)}\nu^{(m)}+\mu^{(f)}\nu^{(f)}+2\mu^{(m)}\nu^{(m)}\nu^{(f)}-2\mu^{(f)}\nu^{(f)}\nu^{(m)} \quad (9)$$

$$c=\left(\mu^{(m)}-\mu^{(f)}\right)\begin{pmatrix}\mu^{(f)}-\mu^{(m)}+\mu^{(f)}\nu^{(f)}-\mu^{(m)}\nu^{(m)}+2\mu^{(m)}\nu^{(f)}- \\ -2\mu^{(f)}\nu^{(m)}+2\mu^{(m)}\nu^{(f)}\nu^{(m)}-2\mu^{(f)}\nu^{(m)}\nu^{(f)}\end{pmatrix} \quad (10)$$

$$g=\left(2-2\nu^{(m)}\right) \quad (11)$$

Assuming the fibre and matrix are both isotropic, Lame constants of both materials are obtained by

$$\lambda=\frac{E}{(1+\nu)(1-2\nu)} \qquad \mu=G. \quad (12)$$

For a composite reinforced by long circular cylindrical fibres, periodically arranged in a square array (Fig. 1) the constants S_i, i = 3, 6, 7 are given as follows [5]

$$S_3=0{,}49247-0{,}47603\xi-0{,}02748\xi^2$$

$$S_6=0{,}36844-0{,}14944\xi-0{,}27152\xi^2$$

$$S_7=0{,}12346-0{,}32035\xi+0{,}23517\xi^2. \quad (13)$$

Further alternative is the periodic microstructure with square arrangement of fibers in the representative volume element (RVE) solved using FEM (Fig. 2).

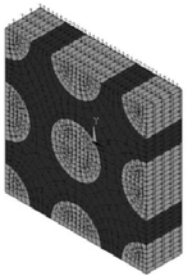

Fig. 2 periodic square microstructure FEA model

The components of the tensor ***C*** are determined solving three elastic models of RVE with parameters (a_1, a_2, a_3) subjected to the periodic boundary conditions. By using a unit value of applied strain, it is possible to compute the stress field, whose average gives the required components of the elastic matrix as

$$C_{ij}=\overline{\sigma}_i=\frac{1}{V}\int_V\sigma_i dV. \quad (14)$$

The coefficients in ***C*** are found by setting a different problem for each column of ***C*** . The elastic properties of the homogenized material can be computed by [5]

$$E_1=C_{11}-2C_{12}^2/\left(C_{22}+C_{23}\right) \quad (15)$$

$$\nu_{12}=C_{12}/\left(C_{22}+C_{23}\right) \quad (16)$$

$$E_2=\left(C_{11}\left(C_{22}+C_{23}\right)-2C_{12}^2\right)\left(C_{22}-C_{23}\right)/\left(C_{11}C_{22}-C_{12}^2\right) \quad (17)$$

$$G_{12}=C_{44} \quad \nu_{23}=\left(C_{11}C_{23}-C_{12}^2\right)/\left(C_{11}C_{22}-C_{12}^2\right) \quad G_{23}=C_{66}. \quad (18)$$

III. Sandwich Plates with Laminate Faces

A sandwich can be defined as a special laminate with three layers. The thin cover sheets, i.e. the layers 1 and 3, have the thicknesses h_1 for the lower skin and h_3 for the upper skin (Fig. 3). The thickness of the core is h_2. In a general case h_1 does not have to be equal to h_3, but in the most important practical case of symmetric sandwiches $h_1 = h_3$.

To formulate the governing differential equations for sandwich plates we draw the conclusion from the similarity of the elastic behaviour between laminates and sandwiches in the first order shear deformation theory and all results derived for laminates can be applied to sandwich plates. We restrict our considerations to symmetric sandwich plates with thin cover sheets.

The assumptions about deformation are:

a) For the sandwich thin cover sheets gilt Kirchhoff´s assumptions about deformation. In-plane stress-strain state is accrued in the sandwich thin cover sheets.

b) The sandwich core with the thickness h_2 transfers only shear stresses perpendicular to the mid-plane of the cover sheets. The material characteristics is the shear modulus G_2.

c) All points in the normal line have the equal deflections $w_1 = w_2 = w_3 = w$.

d) All layers are perfectly bonded.

We can write the shear deformations

$$\gamma_{xz2}=\left(\frac{u_{12}-u_{32}}{h_2}+\frac{\partial w}{\partial x}\right)=\left(\frac{u_1-u_3}{h_2}+\frac{d}{h_2}\frac{\partial w}{\partial x}\right)$$

$$\gamma_{yz2}=\left(\frac{v_{12}-v_{32}}{h_2}+\frac{\partial w}{\partial y}\right)=\left(\frac{v_1-v_3}{h_2}+\frac{d}{h_2}\frac{\partial w}{\partial y}\right) \quad (19)$$

where d is the distance of sheets mid-planes.

$$d=h_2+\frac{h_1+h_3}{2}. \quad (20)$$

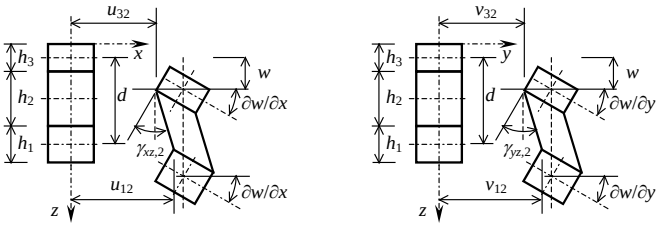

Fig. 3 geometry of deformation

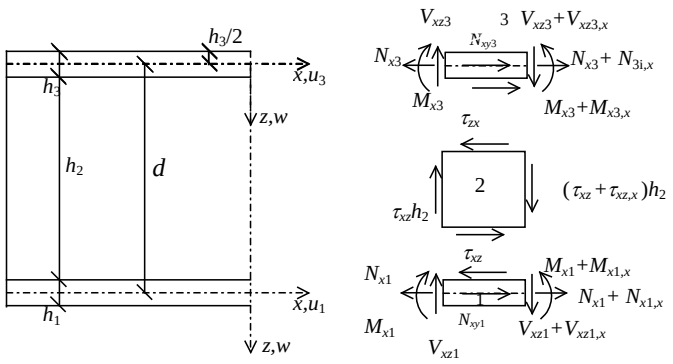

Fig. 4 internal forces at the sandwich element in the (*x*, *z*) plane

Most sandwich structures can be modelled and analyzed using the shear deformation theory for laminate plates [6]. The components of vector of internal forces ***N***, ***M***, ***V*** at the sandwich element in the (*x*, *z*) plane are shown in the Figure 4.

The in-plane resultants ***N*** for sandwiches are defined by

$$\mathbf{N} = \int_{-\left(\frac{1}{2}h_2+h_1\right)}^{-\frac{1}{2}h_2} \boldsymbol{\sigma} dz + \int_{\frac{1}{2}h_2}^{\frac{1}{2}h_2+h_3} \boldsymbol{\sigma} dz. \tag{21}$$

The moment resultants are defined by

$$\mathbf{M} = \int_{-\left(\frac{1}{2}h_2+h_1\right)}^{-\frac{1}{2}h_2} \boldsymbol{\sigma} z dz + \int_{\frac{1}{2}h_2}^{\frac{1}{2}h_2+h_3} \boldsymbol{\sigma} z dz \tag{22}$$

and the transverse shear force by

$$\mathbf{V} = \int_{-\frac{1}{2}h_2}^{\frac{1}{2}h_2} \boldsymbol{\tau} dz. \tag{23}$$

For the resultants ***N*** and ***M*** the integration is carried out over the sheets only and for the transverse shear force over the core.

The constitutive equations for a sandwich are written in the hypermatrix form

$$\begin{pmatrix} \mathbf{N} \\ \mathbf{M} \\ \mathbf{V} \end{pmatrix} = \begin{pmatrix} \mathbf{A} & \mathbf{B} & \mathbf{0} \\ \mathbf{C} & \mathbf{D} & \mathbf{0} \\ \mathbf{0} & \mathbf{0} & \mathbf{A}^s \end{pmatrix} \begin{pmatrix} \boldsymbol{\varepsilon}^0 \\ \boldsymbol{\kappa} \\ \boldsymbol{\gamma} \end{pmatrix}, \tag{24}$$

with stiffness coefficients

$$A_{ij} = A_{ij}^{(1)} + A_{ij}^{(3)}, \qquad B_{ij} = \frac{1}{2}h^{(2)}\left(A_{ij}^{(3)} - A_{ij}^{(1)}\right),$$

$$C_{ij} = C_{ij}^{(1)} + C_{ij}^{(3)}, \qquad D_{ij} = \frac{1}{2}h^{(2)}\left(C_{ij}^{(3)} - C_{ij}^{(1)}\right),$$

$$A_{ij}^s = E_{ij}^s h^{(2)};\ i,j = 4, 5, \tag{25}$$

where E_{ij}^s are the transverse shear moduli of the core.

From equilibrium equations results the set of five differential equations correspond with five partial differential equilibrium equations. For the symmetric sandwich plate element with laminated faces gilt

$$A_{11}^{(1)}\frac{\partial^2 u_1}{\partial x^2} + 2A_{14}^{(1)}\frac{\partial^2 u_1}{\partial x \partial y} + A_{44}^{(1)}\frac{\partial^2 u_1}{\partial y^2} + A_{14}^{(1)}\frac{\partial^2 v_1}{\partial x^2} + \left(A_{12}^{(1)} + A_{44}^{(1)}\right)\frac{\partial^2 u_1}{\partial x \partial y} +$$
$$+ A_{24}^{(1)}\frac{\partial^2 v_1}{\partial y^2} - E_{55}\left(\frac{\partial \overline{w}}{\partial x} - \psi\right) - E_{56}\left(\frac{\partial \overline{w}}{\partial y} - \varphi\right) = 0 \tag{26}$$

$$A_{22}^{(1)}\frac{\partial^2 v_1}{\partial y^2} + \left(A_{12}^{(1)} + A_{44}^{(1)}\right)\frac{\partial^2 u_1}{\partial x \partial y} + A_{24}^{(1)}\frac{\partial^2 u_1}{\partial y^2} + A_{44}^{(1)}\frac{\partial^2 v_1}{\partial x^2} + 2A_{24}^{(1)}\frac{\partial^2 u_1}{\partial x \partial y} +$$
$$+ A_{22}^{(1)}\frac{\partial^2 v_1}{\partial y^2} - E_{56}\left(\frac{\partial \overline{w}}{\partial x} - \psi\right) - E_{66}\left(\frac{\partial \overline{w}}{\partial y} - \varphi\right) = 0 \tag{27}$$

$$A_{11}^{(3)}\frac{\partial^2 u_3}{\partial x^2} + 2A_{14}^{(3)}\frac{\partial^2 u_3}{\partial x \partial y} + A_{44}^{(3)}\frac{\partial^2 u_3}{\partial y^2} + A_{14}^{(3)}\frac{\partial^2 v_3}{\partial x^2} + \left(A_{12}^{(3)} + A_{44}^{(3)}\right)\frac{\partial^2 u_3}{\partial x \partial y} +$$
$$+ A_{24}^{(3)}\frac{\partial^2 v_3}{\partial y^2} + E_{55}\left(\frac{\partial \overline{w}}{\partial x} - \psi\right) + E_{56}\left(\frac{\partial \overline{w}}{\partial y} - \varphi\right) = 0 \tag{28}$$

$$A_{22}^{(3)}\frac{\partial^2 v_3}{\partial y^2} + \left(A_{12}^{(3)} + A_{44}^{(3)}\right)\frac{\partial^2 u_3}{\partial x \partial y} + A_{24}^{(3)}\frac{\partial^2 u_3}{\partial y^2} + A_{44}^{(3)}\frac{\partial^2 v_3}{\partial x^2} + 2A_{24}^{(3)}\frac{\partial^2 u_3}{\partial x \partial y} +$$
$$+ A_{22}^{(3)}\frac{\partial^2 v_3}{\partial y^2} + E_{56}\left(\frac{\partial \overline{w}}{\partial x} - \psi\right) + E_{66}\left(\frac{\partial \overline{w}}{\partial y} - \varphi\right) = 0 \tag{29}$$

$$D_{11}\frac{\partial^4 w}{\partial x^4} + 4D_{14}\frac{\partial^4 w}{\partial x^3 \partial y} + 2\left(D_{12} + 2D_{44}\right)\frac{\partial^4 w}{\partial x^2 \partial y^2} + 4D_{24}\frac{\partial^4 w}{\partial x \partial y^3} +$$
$$+ D_{22}\frac{\partial^4 w}{\partial y^4} - \overline{A}_{55}\left(\frac{\partial^2 \overline{w}}{\partial x^2} - \frac{\partial \psi}{\partial x}\right) - \overline{A}_{56}\left(\frac{\partial^2 \overline{w}}{\partial x \partial y} - \frac{\partial \varphi}{\partial x}\right) -$$
$$- \overline{A}_{65}\left(\frac{\partial^2 \overline{w}}{\partial x \partial y} - \frac{\partial \psi}{\partial y}\right) - \overline{A}_{66}\left(\frac{\partial^2 \overline{w}}{\partial y^2} - \frac{\partial \varphi}{\partial y}\right) = p. \tag{30}$$

The solving of unknown functions $u_1(x,y)$, $u_3(x,y)$, $v_1(x,y)$, $v_3(x,y)$, $w(x,y)$ have to perform the boundary conditions for each boundary. Consistent with the eight order set of differential equations four boundary conditions must be prescribed for each edge of the plate. The classical boundary conditions

N_n or u, N_{nt} or v, M_n or $\partial w/\partial n$,

$$V_n = Q_n + \frac{\partial M_{nt}}{\partial t} \quad \text{or} \quad w \tag{31}$$

must be specified. The subscripts n and t in the boundary conditions above denote the coordinates normal and tangential to the boundary. It is well known that in the classical plate theory the boundary cannot responded separately to the shear force resultant Q_n and the twisting moment M_{nt} but only to the effective or Kirchhoff shear force resultant. Equations (31) may be used to represent any form of simple edge conditions, e.g. clamped, simply supported and free.

If the sandwich layers are symmetrical to the mid-plane, for the simplified form of equations (31), the boundary conditions are

Simply supported edge: $w = 0, \quad M_n = 0$,

Clamped edge: $w = 0, \quad \partial w/\partial n = 0$,

Free edge: $M_n = 0, \quad V_n = 0$.

We have used the finite element method for solving the problem. The continuum was divided to the finite number of rectangular finite plate elements.

IV. Design Optimization

Before starting the topic of design optimization, it is important to distinguish between analysis and design. Analysis is the process of determining the response of a specified system to its environment. Design is the actual process of defining the system. Analysis is therefore a subset of design.

Engineering design is an iterative process. The design is continuously modified until it meets evaluation and acceptance criteria set by the engineer. Mathematical and empirical formulas and experience have been useful in the traditional design processes to verify the adequacy of designs. A fully automated design optimization is used when engineers are trying to modify a design which level of complexity exceeds their ability to make appropriate changes. It is not surprising that even what might appear as extremely simple design task may easily be a real challenge to the designer during the decision-making process.

Design optimization refers to the automated redesign process that attempts to minimize an objective function subject to limits or constraints on the response by using a rational mathematical approach to yield improved designs.

A feasible design is a design that satisfies all of the constraints. A feasible design may not be optimal. An optimum design is defined as a point in the design space for which the objective function is minimized or maximized and the design is feasible.

The optimization process is applied to the approximate problem represented by the polynomial approximation. The coefficients of the polynomial function are determined by the least squares regression.

For regression analysis the singular value decomposition is used. When the objective function and constraints are approximated and their gradients with respect to the design variables are calculated based on chosen approximation, it is possible to solve the approximate optimization problem.

One of the algorithms used in the optimization module is called the Modified Feasible Direction method (MFD). The solving process is iterated until convergence is achieved.

It is important to distinguish the iteration inside the approximate optimization from the loop in the overall optimization process. Figure 5 shows the iterative process within the optimization loop.

Using the modified feasible direction method (MFD) [7, 8] the solving process is iterated until convergence is achieved:

1. $q = 0,\ X^q = X^m$.
2. $q = q+1$.
3. Evaluate objective function and constraints.
4. Identify critical and potentially critical constraints $\overline{N}_c$.
5. Calculate gradient of objective function $\nabla F(X_i)$ and constraints $\nabla g_k(X_i)$, where $k = 1,2,...,\overline{N}_c$.
6. Find a usable-feasible sear ch direction S^q.
7. Perform a one-dimensional search $X^q = X^{q-1} + \alpha S^q$.
8. Check convergence. If satisfied, make $X^{m+1} = X^q$. Otherwise, go to 2.
9. $X^{m+1} = X^q$.

Convergence of MFD to the optimum is checked by criteria of maximum iterations and criteria changes of objective function.

Besides the previously mentioned criteria, the Kuhn-Tucker conditions necessary for optimality must be satisfied.

The other algorithm for solving the nonlinear approximate optimization problem is called the Sequential Linear Programming method (SLP). The iterative process of SLP within each optimization loop is shown below:

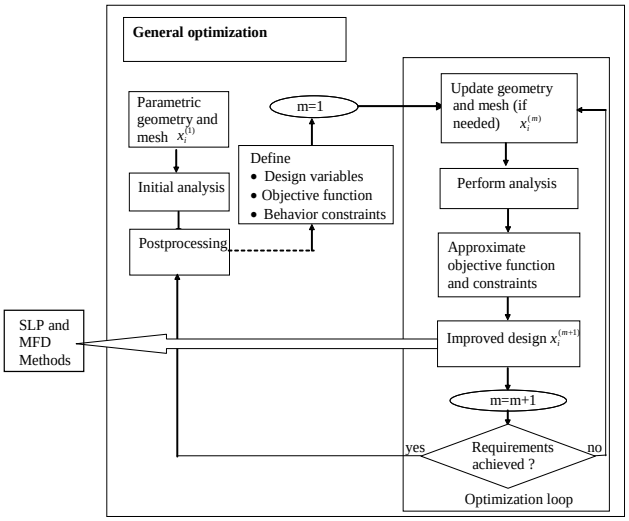

Fig. 5 general optimization process

1. p=0, X^p=X^m.
2. p=p+1.
3. Linearize the problem at X^{p-1} by creating a first order Taylor Series expansion of the objective function and retained constraints

$$F(X) = F(X^{p-1}) + \nabla F(X^{p-1})(X - X^{p-1})$$

$$g(X) = g(X^{p-1}) + \nabla g(X^{p-1})(X - X^{p-1}).$$

4. Use this approximation of optimization instead of the original nonlinear functions:

Maximize: $F(X)$

Subject to: $g(X) \le 0$ and $\overline{X}_i^L \le X_i \le \overline{X}_i^U$.

5. Find an improved design X^p (using the Modified Feasible Direction method).
6. Check feasibility and convergence. If both of them are satisfying, go to 7. Otherwise, go to step 2.
7. $X^{m+1} = X^p$.

Using the SLP method the solving process is iterated until convergence is achieved. Convergence or termination checks are performed at the end of each optimization loop in general optimization. The optimization process continues until either convergence or termination occurs.

The process may be terminated before convergence in two cases:

- the number of design sets so far exceeds the maximum number of optimization loops,
- if the initial design is infeasible and the allowed number of consecutive infeasible designs has been exceeded.

V. Modeling of Sandwich Plates and Numerical Solution

For the numerical solution the simply supported panel with laminate facings was used. Panel length is 3750 mm, nominal width is 1000 mm. Thickness of the facings is h_1=h_3 and core is h_2 (Fig. 6). On the panel affects uniform static wind load with intensity of 2 kPa in the bending plane. The laminate Carbon/epoxy facings are composed of eight identical thickness layers of a symmetric laminate $[0/\pm45/90]_s$.

It was considered the carbon fibres in epoxy matrix, while unidirectional laminate layer has characteristics:

E_f = 230 GPa; E_m = 3 GPa; ν_f = 0.2; ν_m = 0.3; V_f = 0.6; ρ_k = 1580 kg/m^3.

Sandwich core, consisting of PUR foam, has material constants: E_{PUR} = 16 MPa; ν_{PUR} = 0.3; ρ_{PUR} = 150 kg/m^3.

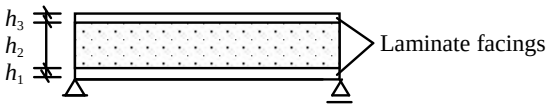

Fig. 6 scheme of sandwich structure

VI. Results

Laminate properties were determined by homogenization techniques [9, 14]. Computational program MATLAB was used to calculate the effective material properties of laminate facings (Figs. 7-10).

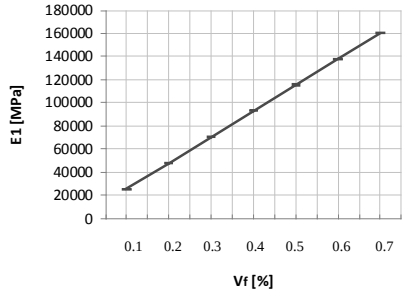

Fig. 7 longitudinal modulus E_1 versus fiber volume fraction

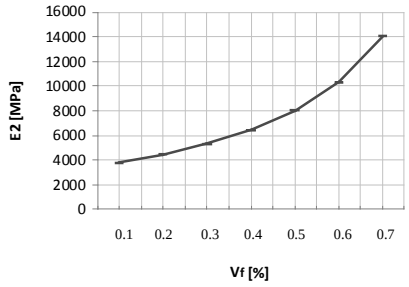

Fig. 8 transversal modulus E_2 versus fiber volume fraction

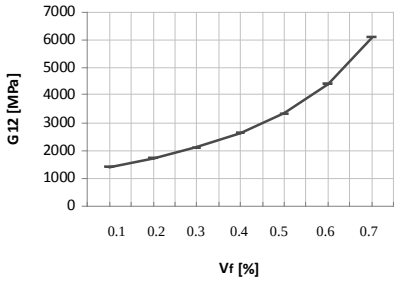

Fig. 9 shear modulus G_{12} versus fiber volume fraction

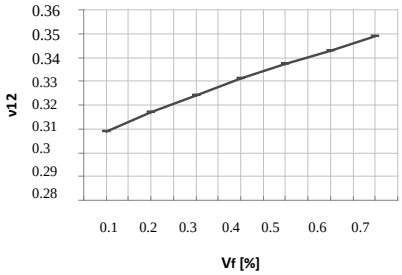

Fig. 10 Poisson ratio ν_{12} versus fiber volume fraction

Numerical experiments were conducted through the COSMOS/M program.

There were solved three optimization processes:

The design optimization problem 1 can be written as follows:

$$F(\boldsymbol{X}) = G(h_1) \rightarrow \min \quad [\mathrm{N}]$$
$$1\cdot10^{-4} \le h_1 \le 0.01 \quad [\mathrm{m}]$$
$$0 \le w \le 0.0375 \quad [\mathrm{m}]$$

The initial values and bounds of design variables, constraints and the objective function are shown in the Table 1.

Optimization parameters		Initial values	Final values	Tolerance τ
Design variable	h_1 [m]	0.001	$5.683\cdot10^{-4}$	$1\cdot10^{-5}$
Objective function	G [N]	573.75	568.893	$1\cdot10^{-3}$
Constraint	w [m]	0.0238	0.0375	$3.75\cdot10^{-4}$

Table 1 summary of results of the optimization problem 1

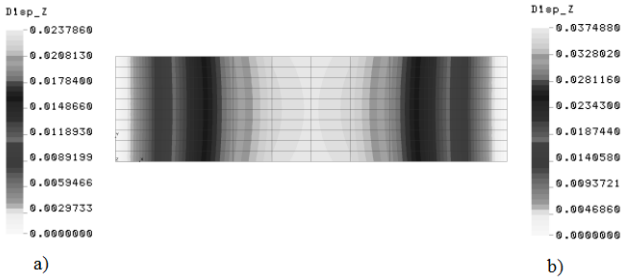

Fig. 11 deflections w before - a) and after - b) optimization process 1

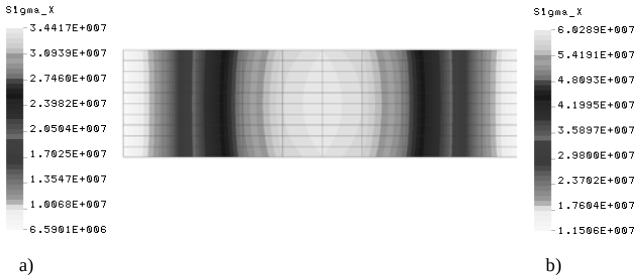

a) b)

Fig. 12 effective stresses σ_x at the bottom of first layer before - a) and after - b) optimization process 1

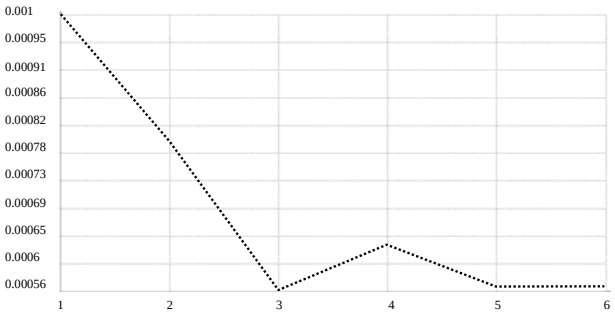

Fig. 13 variation of design variable h_1 [m] - optimization process 1

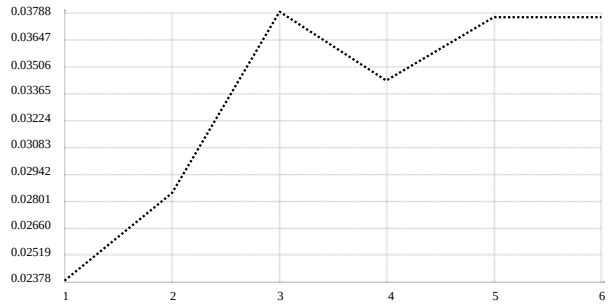

Fig. 14 variation of constraint values w [m] - optimization process 1

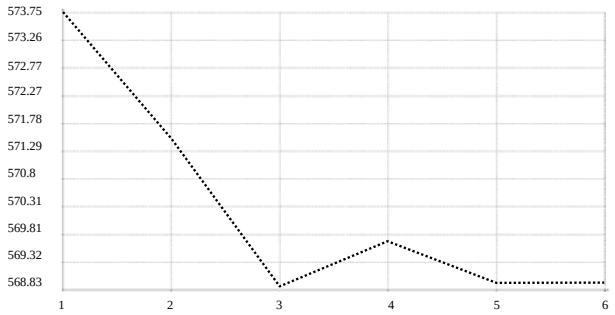

Fig. 15 variation of objective function values G [N] - optimization process 1

The design optimization problem 2 can be written as follows:

$$F(\boldsymbol{X}) = G(h_2) \rightarrow \min \quad [\mathrm{N}]$$

$$1 \cdot 10^{-2} \le h_2 \le 0.2 \ [\mathrm{m}]$$

$$0 \le w \le 0.0375 \quad [\mathrm{m}]$$

The initial values and bounds of design variables, constraints and the objective function are shown in the Table 2 for optimization problem 2.

Optimization parameters		Initial values	Final values	Tolerance τ
Design variable	h_2 [m]	0.1	$7.755 \cdot 10^{-2}$	$1 \cdot 10^{-5}$
Objective function	G [N]	573.75	447.445	$1 \cdot 10^{-3}$
Constraint	w [m]	0.02378	0.0375	$3.75 \cdot 10^{-4}$

Table 2 summary of results of the optimization problem 2

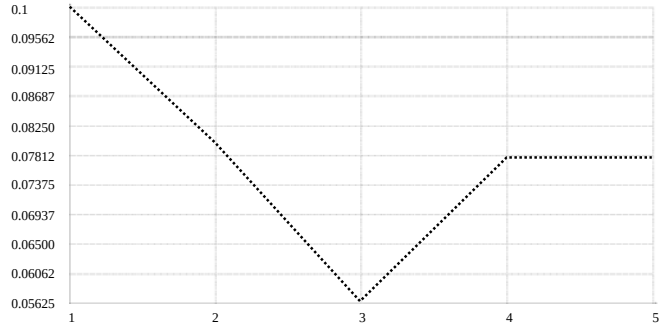

Fig. 16 variation of design variable h_2 [m] during the optimization process 2

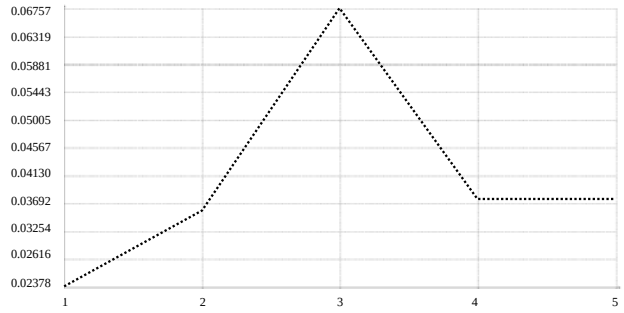

Fig. 17 variation of constraint values w [m] during the optimization process 2

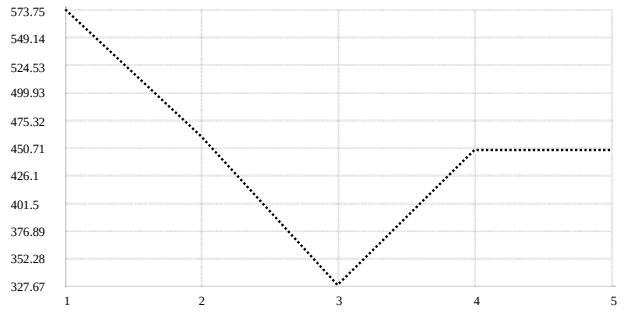

Fig. 18 variation of objective function values G [N] during the optimization process 2

The design optimization problem 3 can be written as follows:

$$F(\boldsymbol{X}) = G(h_1, h_2) \rightarrow \min \quad [\mathrm{N}]$$

$$5 \cdot 10^{-4} \le h_1 \le 0.002 \ [\mathrm{m}]$$

$$5 \cdot 10^{-2} \le h_2 \le 0.2 \quad [\mathrm{m}]$$

$$0 \le w \le 0.0375 \quad [\mathrm{m}]$$

The initial values and bounds of design variables, constraints and the objective function are shown in the Table 3 for optimization problem 3.

Optimization parameters		Initial values	Final values	Tolerance τ
Design variable	h_1 [m]	0.001	0.002	$1\cdot10^{-5}$
Design variable	h_2 [m]	0.158	0.05067	$1\cdot10^{-5}$
Objective function	G [N]	900	341.31	$1\cdot10^{-3}$
Constraint	w [m]	0.01092	0.0375	$3.75\cdot10^{-4}$

Table 3 summary of results of the optimization problem 3

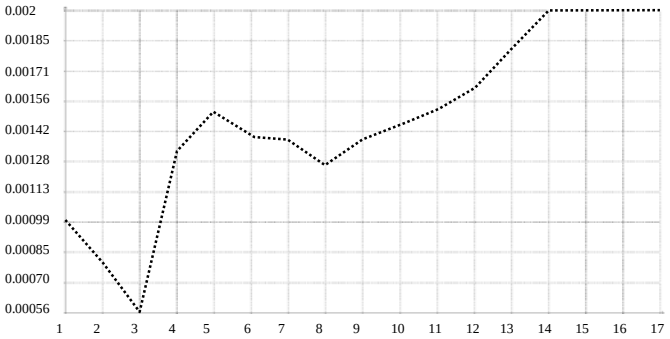

Fig. 19 variation of design variables h_1 [m] during optimization process 3

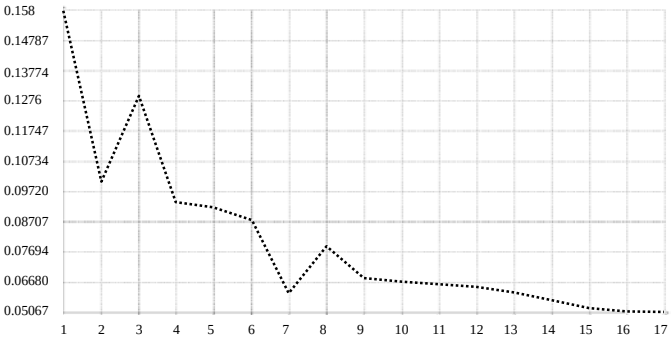

Fig. 20 variation of design variables h_2 [m] during optimization process 3

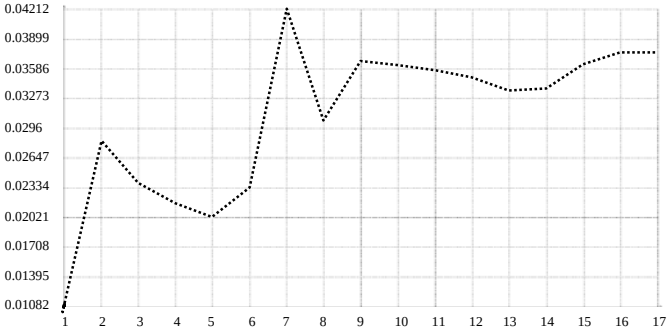

Fig. 21 variation of constraints values w [m]during optimization process 3

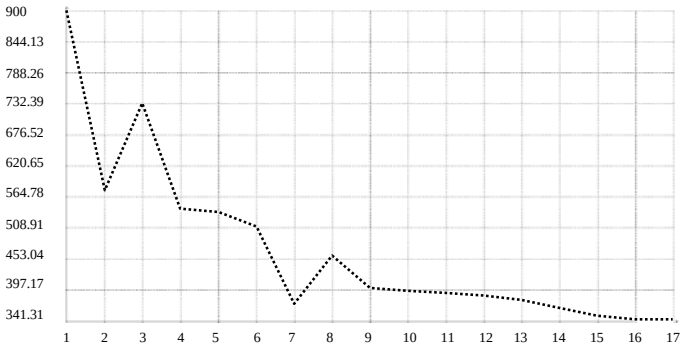

Fig. 22 variation of objective function values G [N] during optimization process 3

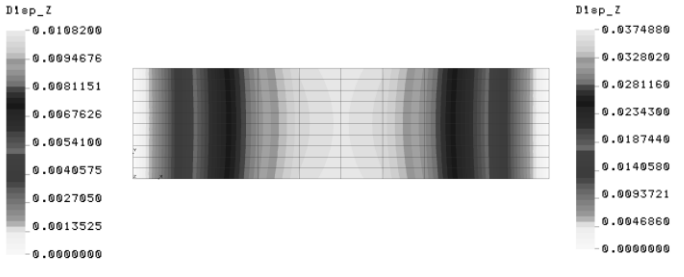

Fig. 23 Contour plot of deflections w before and after the optimization process 3

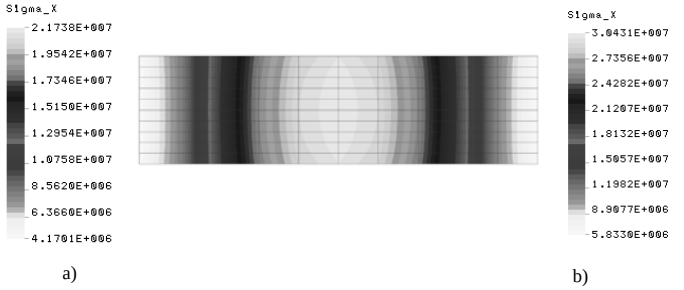

Fig. 24 contour plot of stresses σ_x at the bottom of the first layer before and after the optimization process 3

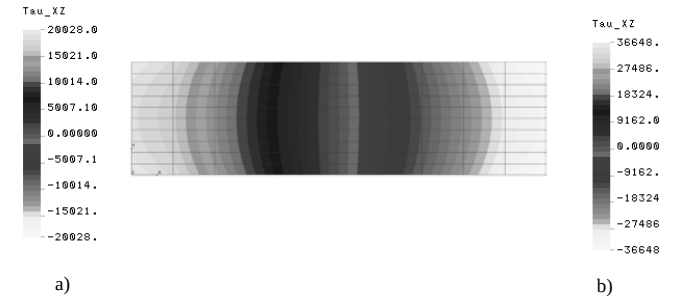

Fig. 25 contour plot of stresses τ_{xz} at the bottom of core layer before and after the optimization process 3

VII. Discussion and Conclusion

The homogenization techniques applied for periodical RVE was used to get the material characteristics of outer laminate layers of sandwich structure (Figs. 7-10) [17, 19, 20].

The first order shear laminate theory was used by the FEM analysis of the problem [10-14]. The optimization problem

was formulated as a minimum weight of simply supported rectangular sandwich plate subject to deflection constraint in the middle of the plate. Design variables were thicknesses h_1= h_3 and h_2 of sandwich layers. The optimal problem was solved using SLP and MFD method [15, 18] with maximum 70 iterations in each own optimization loop. In the Figs. 13-22 there are depicted variations of design variables, constraint and objective function during the optimization process 1, 2 and 3, respectively. Initial and final values of optimization parameters for optimization process 1, 2 and 3 are shown in the Tables 1, 2 and 3, respectively. Contour plot of deflections *w*, stresses σ_x at the bottom of the first layer before and after optimization process 1 are illustrated in the Figs. 11 and 12, respectively. Contour plot of deflections *w*, stresses σ_x at the bottom of the first layer and stresses τ_{xz} at the bottom of the core layer before and after optimization process 3 are illustrated in the Figs. 23-25, respectively. General optimization procedure is optimization process 3 with two design variables, where designer can optimize whole thickness of sandwich panel within taking into account both constraints for thicknesses h_1 and h_2. A hygrothermal effect of environment was not taken into account. Only static analysis under mechanical loading of sandwich multilayered structure was performed [21].

ACKNOWLEDGMENT

This work was supported by the Scientific Grant Agency of the Ministry of Education of Slovak Republic and the Slovak Academy of Sciences under Project VEGA 1/0477/15.

REFERENCES

[1] H. Altenbach, J. Altenbach, W. "Kissing, Structural analysis of laminate and sandwich beams and plates," Lublin, 2001.

[2] R. Dhabale, V. S. Jatti, "Optimization of material removal rate of AlMg1SiCu in turning operation using genetic algorithm", WSEAS Transactions on Applied and Theoretical Mechanics, Volume 10, pp. 95-101, 2015.

[3] A.M. Valuev, "Models and methods of multiobjective optimization in problems of quarry design and planning", WSEAS Transactions on Mathematics, Volume 13, pp. 557-566, 2014.

[4] E.A. Vorontsova, "A projective separating plane method with additional clipping for non-smooth optimization", WSEAS Transactions on Mathematics, Volume 13, pp. 115-121, 2014.

[5] E. J. Barbero, "Finite element analysis of composite materials," CRC Press, USA, ISBN-13: 978-1-4200-5433-0, 2007.

[6] Z. Gürdal, R.T. Haftka, P. Hajela, "Design and Optimization of Laminated Composite Materials," J. Wiley & Sons, 1999.

[7] E. Kormanikova, I. Mamuzic, "Buckling analysis of a laminate plate," Metalurgija. Vol. 47, no. 2 (2008), pp. 129-132. - ISSN 0543-5846.

[8] M. Mihalikova [et al.], "Influence of strain rate on automotive steel sheet breaking," Chemické listy. Vol. 105, no. 17 (2011), pp. 836-837. - ISSN 0009-2770.

[9] J. Sykora, M. Sejnoha, J. Sejnoha, "Homogenization of coupled heat and moisture transport in masonry structures including interfaces," Applied Mathematics and Computation, 219 (13), pp. 7275-7285, 2013.

[10] S. Harabinova, E. Panulinova, "Properties of Aggregates of Steel-Making Slag," GeoConference on Energy and Clean Technologies: conference proceedings, Albena, Bulgaria – Sofia, Volume 2, 2014, pp. 199-202.

[11] N. Jendzelovsky, "Analysis of the 3D state of stress of a concrete beam," Advanced Materials Research, Volume 969, pp. 45-50, 2014.

[12] K. Tvrda, "Probability and sensitivity analysis of plate," Applied Mechanics and Materials, Volume 617, pp. 193-196, 2014.

[13] M. Krejsa, P. Janas, I. Yilmaz, M. Marschalko, T. Bouchal, "The use of the direct optimized probabilistic calculation method in design of bolt reinforcement for underground and mining workings," The Scientific World Journal, Volume 2013, Article number 267593, 2013.

[14] M. Zmindak, Z. Pelagic, M. Bvoc, "Analysis of high velocity impact on composite structures," Applied Mechanics and Materials, Volume 617, pp. 104-109, 2014.

[15] J. Kralik, "Optimal design of npp containment protection against fuel container drop", Advanced Materials Research, Volume 688, pp. 213-221, 2013.

[16] J. Melcer, G. Lajcakova, "Comparison of finite element and classical computing models of reinforcement pavement," Advanced Materials Research, Volume 969, pp. 85-88, 2014.

[17] M. Sejnoha, J. Zeman, "Micromechanical modeling of imperfect textile composites," (2008) International Journal of Engineering Science, 46 (6), pp. 513-526.

[18] E. Kormanikova, I. Mamuzic, "Optimization of laminates subjected to failure criterion," Metalurgija, vol. 50 (1), pp. 41-44, 2011.

[19] J. Ma, S. Sahraee, P. Wriggers, , L. De Lorenzis, "Stochastic multiscale homogenization analysis of heterogeneous materials under finite deformations with full uncertainty in the microstructure", Computational Mechanics, Volume 55, Issue 5, 25 May 2015, Pages 819-835.

[20] C. Maruccio, L. De Lorenzis, L. Persano, D. Pisignano, "Computational homogenization of fibrous piezoelectric materials", Computational Mechanics, Volume 55, Issue 5, 8 April 2015, Pages 983-998.

[21] S. Tang, Y. Yang, X. H. Peng, X. X. Huang, K. Elkhodary, "A semi-numerical algorithm for instability of compressible multilayered structures", Computational Mechanics, Volume 56, Issue 1, 22 April 2015, Pages 63-75.

E. Kormanikova graduated at the Technical University of Košice, Civil Engineering Faculty, study program - Building Construction. After finishing the university she started to work at the Technical University of Košice, Civil Engineering Faculty, Department of Structural Mechanics. Since 2009 she has worked at Civil Engineering Faculty, Technical University of Košice, study program - Theory and Design of Engineering Structures, as associate professor. Her research topic is design and optimization of structural elements and structures made of composite materials.

K. Kotrasova graduated at the Technical University of Košice, Civil Engineering Faculty, study program - Building Construction. After finishing of the university she started to work at RCB in Spišská Nová Ves as designer and then at the Technical University of Košice, Faculty of Mechanical Engineering, study program - Applied Mechanics. The research topics: seismic design of liquid storage ground-supported composite tanks, interaction problems of fluid, solid and subsoil.